N66 24631

# 24. WIND-TUNNEL BOUNDARY INTERFERENCE FOR V/STOL TESTING

By Harry H. Heyson and Kalman J. Grunwald

NASA Langley Research Center

## SUMMARY

The wake skew angle used in applying the theory of NASA TR R-124 to data correction should be such that the angular deflection of the wake vorticity from the horizontal is one-half that calculated from momentum theory at the lifting element. This usage is in contrast to that of the original paper which used the angle of the mass flow. Because of large-scale recirculation effects, there is a finite lower limit to the test speed at which reliable and correctable data can be obtained in closed wind tunnels. Although a zero-correction wind tunnel for V/STOL testing has not yet been achieved, it is shown that the use of suitably mixed wind-tunnel boundaries can alleviate boundary effects on V/STOL data.

24

## INTRODUCTION

The very slow speed regimes of flight give the aerodynamicist some of his most difficult problems. The small perturbation assumptions inherent in almost all configuration studies begin to break down, and extreme interferences appear to exist between the various aerodynamic components of the aircraft. As a result, the wind tunnel is almost the only means of determining, even approximately, the performance and stability of the entire aircraft.

Unfortunately, wind-tunnel results are not identical to the results obtained in flight because of the wind-tunnel boundaries in close proximity to the model. The purpose of the present paper is to examine experimentally the adequacy of current theory in predicting the effect of the wind-tunnel boundaries on the data from specific models. In addition, some information is presented on the degree of relief from corrections which can be obtained by appropriate slotting and opening of the wind-tunnel walls.

The present paper is limited to the effect of the wind-tunnel boundaries upon model data. In particular, no attempt is made to evaluate the problems of scaling or model detailing on the extrapolation of model data to full-scale Reynolds numbers.

## SYMBOLS

$A_M$ momentum area of lifting system

$A_T$ cross-sectional area of wind-tunnel test section

$B$ semiwidth of wind-tunnel test section

$C_L$ lift coefficient, $L/qS$

$C_{N,t}$ tail normal-force coefficient, $\frac{\text{Tail normal force}}{qS}$

$C_\mu$ jet momentum coefficient, $\frac{(\text{Jet mass flow})(V_j)}{qS}$

$\Delta C_\mu$ difference between corrected and uncorrected values of $C_\mu$

$\bar{c}$ mean aerodynamic chord

$H$ semiheight of wind-tunnel test section

$L$ lift

$M_Y$ pitching moment, positive nose up

$q$ dynamic pressure

$R$ rotor radius

$S$ wing area

$T_s$ static thrust

$V$ tunnel velocity

$V_j$ jet velocity

$V_{j,s}$ jet velocity in static thrust

$u_o$ mean or momentum-theory value of longitudinal induced velocity at model, positive rearward

$\Delta u_D$ longitudinal interference velocity due to drag, positive rearward

$\Delta u_L$ longitudinal interference velocity due to lift, positive rearward

$w_o$ mean or momentum-theory value of vertical induced velocity at model, positive upward

$\Delta w$ vertical interference velocity (general), positive upward

$\Delta w_D$ vertical interference velocity due to drag, positive upward

$\Delta w_L$ vertical interference velocity due to lift, positive upward

$x$ distance rearward from center of lift

$\alpha$ angle of attack

$\Delta\alpha$ correction to angle of attack resulting from presence of wind-tunnel boundaries

$\gamma$ ratio of wind-tunnel width to wind-tunnel height, B/H

$\delta$ jet-boundary correction factor, defined by equation $\Delta\alpha = \delta \frac{S}{A_T} C_L$; also, jet-boundary correction factor (general)

$\delta_{u,D}$ correction factor for longitudinal interference due to drag, defined by equation $\Delta u_D = \delta_{u,D} \frac{A_M}{A_T} u_o$

$\delta_{u,L}$ correction factor for longitudinal interference due to lift, defined by equation $\Delta u_L = \delta_{u,L} \frac{A_M}{A_T} w_o$

$\delta_{w,D}$ correction factor for vertical interference due to drag, defined by equation $\Delta w_D = \delta_{w,D} \frac{A_M}{A_T} u_o$

$\delta_{w,L}$ correction factor for vertical interference due to lift, defined by equation $\Delta w_L = \delta_{w,L} \frac{A_M}{A_T} w_o$

$\chi$ angle between vertical and angle of wake at model

$\chi_{eff}$ effective skew angle, $\frac{\chi + 90^\circ}{2}$

## RESULTS AND DISCUSSION

### Review of Theory

The classical corrections to wind-tunnel data (for example, ref. 1) are applied according to the equation

$$\Delta\alpha = \delta \frac{S}{A_T} C_L \tag{1}$$

Equation (1) appeared to present considerable difficulty when VTOL models were first tested in wind tunnels. The problem was that, as the wind-tunnel velocity was decreased at constant lift, the lift coefficient increased without bound, and the correction angle approached infinity. As a point of fact, the problem was never really quite this serious. Equation (1) was derived by obtaining the vertical interference velocity and then assuming that the correction angle was small enough so that the angle and its tangent were equal. Without this final assumption, equation (1) would have been

$$\tan \Delta\alpha = \frac{\Delta w}{V} = \delta \frac{S}{A_T} C_L \qquad (2)$$

In equation (2), as the wind-tunnel speed approaches zero, the lift coefficient at constant lift still approaches infinity; however, the correction angle only approaches 90°. In other words, if the tunnel velocity (V) is zero, a closed wind tunnel still produces an upwash ($\Delta w$) in the vicinity of a lifting model. Unfortunately, the assumption lying behind the calculation of the correction factor $\delta$, namely that the wake passes directly downstream along the wind-tunnel axis, is severely violated at very low and zero wind-tunnel velocities. Thus, usable results cannot be anticipated from the application of either equation (1) or (2) to tests of VTOL models.

A more recent analysis made at the Langley Research Center (refs. 2 and 3) treats the case where the wake is deflected substantially downward from the model. This theory obtains corrections in the form of interference velocities that are functions of the wake skew angle. (See fig. 1.) It will be observed that, in general, both horizontal and vertical interference velocities are obtained as a result of both lift and drag. In actually applying corrections to data, these interference velocities are used to obtain a new corrected angle of attack and a new effective forward velocity.

The correction factors describing the interference velocities have been calculated and tabulated for a wide range of variables (refs. 4 to 7). A sample case for the center of lift in a closed wind tunnel having a width-height ratio of 1.5 is presented in figure 2. The correction factor that corresponds to the classical correction factor is $\delta_{w,L}$. At $\chi = 90°$, it differs from the classical correction factor only by a factor of -4, which occurs solely because of the difference in definition. Furthermore, at $\chi = 90°$, all the other correction factors are zero. Thus, the classical theory is contained as a subcase of the new theory. It will be observed, however, that when the wake is deflected substantially downward, the vertical interference due to lift increases substantially, and in addition, a smaller upwash due to drag is encountered. Furthermore, both lift and drag contribute, in general, to a reduction in effective forward velocity.

## Earlier Experimental Studies

Over the past several years investigators at the Langley Research Center have conducted experimental studies of the adequacy of the new theory by testing tilt-wing (ref. 8) and fan-in-fuselage (ref. 9) models in different size wind tunnels. Other investigators have tested rotors in wind-tunnel inserts (ref. 10). The tunnels have ranged from about 15 to over 1600 square feet in area. In general, substantially improved agreement was obtained in all cases, with a tendency toward overcorrection at the most severe lift coefficients.

At this point a fan-in-wing model was tested in both a 7- by 10-foot wind tunnel and a 30- by 60-foot wind tunnel (ref. 11). This model was the first model with a tail to which this theory was applied. Once more the theory corrected the model lift and drag reasonably well; however, the calculated correction to the pitching moment was approximately equal, but opposite in sign, to that required to bring the two sets of data into agreement. Obviously, there was an unexplained factor in the application of the corrections.

## Location of the Wake

Before proceeding further, it is well to inquire into the fundamental question of the actual location of the wake. Fortunately, some information on this subject already exists. For example, figure 3 shows the measured vorticity distribution in the wake of a helicopter rotor (ref. 12). The wake of a rotor is usually represented for purposes of calculation as a series of concentric vortex cylinders whose strength is proportional to the local disk-load distribution. Thus it would be expected that, in the survey plane of figure 3, the vorticity would be found to be concentrated within the intersection of these vortex cylinders and the survey plane. (This intersection is shown by the dashed ellipse in fig. 3.) The figure shows that the expected result is not obtained. The dominant feature of the vorticity distribution is the presence of two large, and already well rolled-up, vortices behind the outermost portions of the rotor. It is notable that these vortices are deflected downward only about one-half as far as indicated by momentum theory. This behavior is in contrast to that of the wake mass flow which behaves essentially as indicated by momentum theory.

Joppa (ref. 13), of the University of Washington, starting from the analysis of reference 14, has been able to show theoretically that for low-aspect-ratio wings the result is essentially identical to the previous observation. That is, the final wake vorticity is deflected through approximately one-half of the angle calculated at the wing, rather than through twice the angle as predicted (for the wake mass flow) by linearized theory.

## Effective Wake Skew Angle

The calculation of wind-tunnel boundary corrections may be accomplished by the use of suitably arranged image systems around the real test section. It will be observed that these image systems are comprised of the wake vorticity

rather than the wake mass flow. Furthermore, when the effects of all the image wakes are added, it will be observed that the calculated results are largely produced by image wakes which are at a substantial distance from the model. Thus, the far portions of the wake have a proportionately larger effect on the model (insofar as wall interference is concerned) than does the small portion of the wake immediately near the model. Therefore, it is proposed that a skew angle yielding just one-half the downward angular displacement of momentum theory (such as ref. 15) be used in applying the corrections of reference 2 to wind-tunnel data. In terms of skew angle, the effective skew angle $\chi_{eff}$ is

$$\chi_{eff} = \frac{\chi + 90^\circ}{2} \tag{3}$$

It is recognized that equation (3) cannot be correct in hovering or at extremely low forward speeds. This is evident since in true hovering the skew angle, whether based on wake vorticity or on wake mass flow, is indeed $0^\circ$ and not $45^\circ$ as would be indicated by equation (3). On the other hand, there are limitations on the minimum speed at which tests can be made in a meaningful fashion in wind tunnels, and it is believed that these limitations will generally be encountered before the failure of equation (3). In any event, it appears that the effective skew angle is a superior approximation to the actual wake over the bulk of reasonable test conditions.

## Jet-Flap Model

Recently, data have been obtained for a jet-flap model (fig. 4) in the Langley 300-MPH 7- by 10-foot tunnel as well as in a small wind tunnel 2.70 feet high and 1.88 feet wide. (These wind tunnels are designated 7' × 10' and 2.70' × 1.88' herein.) The model was equipped with a sensitive tail balance, which measured tail normal force, and also was equipped with the usual sting balance, which was arranged so as to measure only the forces on the wing. Roughness strips were applied to both the wing and the tail surfaces to minimize Reynolds number effects.

A sample of the data obtained with this model is shown in figure 5. Corrections have been applied to the data from both wind tunnels. (The corrections to the 7' × 10' wind-tunnel data are very small, on the order of several tenths of a degree; consequently, the uncorrected data are not shown.) The corrections used are those of reference 2 with finite-span effects (for uniform loading) on both wing and tail accounted for by the superposition methods outlined in that paper. Inclusion of the finite-span effects substantially improves the correlation. The small differences in $C_\mu$ resulting from the horizontal interference velocities have been removed from the lift data (fig. 5(a)) by finding $dC_L/dC_\mu$ from closely spaced test runs in the 7' × 10' wind tunnel and then subtracting an amount equal to $(dC_L/dC_\mu)\Delta C_\mu$ from the lift coefficient. In the case of the tail normal force, the behavior of $dC_{N,t}/dC_\mu$ was very erratic with respect to both $C_\mu$ and $\alpha$; consequently, no similar correction has been

applied to the tail-normal-force data. (See fig. 5(b).) The actual changes in $C_\mu$ as a result of the horizontal interference were small for this model.

In addition, no correction has been made to the data to account for the effective aerodynamic warpage of the model as a result of the nonuniformity of the wall-induced interference over the model. In particular, the tail location is aerodynamically equivalent to a tail location that is slightly different from the actual geometric location on the physical model. Also neglected is the vertical motion of the tail in the wind tunnel as the model angle of attack is changed by pivoting about the quarter-chord.

Despite the unaccounted-for features mentioned, it is evident that the application of corrections according to reference 2 has greatly improved the correlation between the data from the two wind tunnels. This trend is particularly evident in the stall angle of attack of the wing at $C_\mu = 1.5$. In the corrected data, the stall angle is reproduced faithfully in both wind tunnels, despite the fact that the wall-induced interference is about 10 percent greater at the wing tips than it is at the center of the model. The improved agreement is equally obvious in the fidelity with which the angle for reversal of tail normal force is reproduced in the corrected data at $C_\mu = 5.0$.

The trend of greatly improved agreement is evident throughout the study except for the highest momentum coefficient at which tests were made. Data for this case ($C_\mu = 10$) are shown in figure 6. The corrected lift coefficients obtained in the two wind tunnels are in reasonable agreement up to an angle of attack of about $10^\circ$, after which the two sets of data diverge. Since the tail normal-force data have substantial scatter and the corrections are large, these data are also in reasonable agreement up to an angle of attack of approximately $10^\circ$, after which these two sets of data also diverge. The physical reason for this divergence is discussed in a subsequent section of this paper.

## Effect of Finite Span

As previously mentioned, inclusion of finite-span effects substantially improves the agreement between the two wind tunnels. In the 7' × 10' wind tunnel, of course, the 1-foot-span model is a reasonably good representation of a vanishingly small model in comparison to the 10-foot width of the tunnel. On the other hand, the 1-foot-span model in the 1.88-foot width of the small wind tunnel cannot be considered vanishingly small under any circumstances. It was for this reason that finite-span effects were included. The importance of including these effects can be seen by comparing figures 7 and 8 with figures 5 and 6. The data of figures 7 and 8 were corrected by using the correction factors for a zero-span model. It is evident from this comparison that it is necessary to include finite-span effects if complete correction of data is desired.

## Jet Thrust

It will be observed that (depending on the value of $C_\mu$) from 40 to over 70 percent of the lift of the jet-flap model is due to the direct thrust of the

compressible jet at the trailing edge of the wing. All the jet thrust was included in the lift coefficient when correcting the data. The close correlation between the two sets of data after correction indicates that, as assumed in references 2 and 3, the exact nature of the lifting system is inconsequential, whether it be propeller, rotor, wing, fan, or jet. The only feature of the configuration that is significant is the distribution of lift and drag within the wind tunnel.

The foregoing comments are reinforced by the information presented in paper no. 13 by Richard J. Margason. In that paper it is shown that even the wake of a direct, circular, compressible jet rapidly rolls up into a subsonic vortex pair when operated in transition. Thus, the application of corrections to such jets should require little or no change in procedure.

## Fan-In-Wing Model

Pitching-moment data from a fan-in-wing model have been mentioned previously in this paper. The model is shown in figure 9. The pitching-moment data from both the 7' × 10' and 30' × 60' wind tunnels are shown in figure 10 as it was originally presented in reference 11. The curve labeled "7' × 10', corrected" was obtained by applying the corrections of reference 2 in accordance with $\chi$ rather than $\chi_{eff}$. It will be observed that the correction displaces the pitching-moment data in a direction opposite to that required in order to correlate the data from the two wind tunnels.

The same data corrected according to reference 2, but with the use of the effective skew angle, are shown in figure 11. The corrections as applied in this case are extremely crude. It is assumed that the model is vanishingly small. Obviously, the 64.5-inch-span model is not small in the 7' × 10' wind tunnel. Examination of the results of reference 2 indicates that this assumption in the present case overestimates the required correction. The effect of the flow distortion over the rear portion of the fuselage (which has substantial area and moment compared with the relatively small tail plane) has also been neglected. This assumption would result in a smaller correction. In the absence of measurements of the load distribution between the fans and the wing, it has been assumed that the load is carried entirely upon the fans. In practice, of course, the wing does carry substantial lift, and two wakes, at different skew angles, exist in the wind tunnel. If the lift distribution between the two lifting systems was accounted for, the upwash at the tail would be reduced. In addition, the vertical displacement of the tail from the wing plane, as well as the large motion of the tail within the wind tunnel as a result of changes in angle of attack, has been neglected. Furthermore, no camber effects on the wing and no pitching-moment changes due to induced flow gradient on the fans were considered.

In addition to the foregoing assumptions, all the data shown herein for this model were obtained at speeds far below an apparently limiting lower speed for VTOL tests in closed wind tunnels. This limit will be discussed in a subsequent section of this paper.

As a result of the factors mentioned previously, the close correlation of the corrected pitching moments is fortuitous. Actually, unpublished tail-off data from both the 7' × 10' and 30' × 60' wind tunnels indicate that the effect of the walls on the pitching moment due to the tail is quite small. Examination of the circulatory flow discussed in a subsequent section indicates that the result of such flow should largely counteract the wall-induced upwash at the tail in this particular test. On the other hand, figure 11 does indicate, at least, that the correction is not in the wrong direction as it appeared to be when calculated with the use of $\chi$ instead of $\chi_{eff}$ (as in fig. 10).

The change in the correction by changing to the effective skew angle may be explained by examination of figure 12. This figure shows the variation of $\delta_{w,L}$ (which in this case is the most significant correction factor) along the longitudinal axis of the model. Note that in correcting pitching moments the problem is generally one of correcting the contribution of the tail to coincide with the tail moment that would be obtained at the conditions to which the lifting system has already been corrected. Thus, it is the relative difference between, rather than the absolute values of, the correction at the center of lift and the tail which is of interest. At $\chi = 0^\circ$, which approximates the original skew angles for the fan-in-wing model, it will be seen that there is a lesser upwash at the tail than at the wing. Thus the tail is working with less lift in the wind tunnel than if it were at the same condition as the wing. To correct for this situation, an appropriate amount of lift must be added to the tail to make the moment more negative as in figure 10. On the other hand, for $\chi = 45^\circ$, which approximates the effective skew angle for this case, the tunnel produces more upwash at the tail than at the center of lift. Consequently, correction makes the moment more positive (fig. 11).

## Tilt-Wing Model

The earlier studies of wall effects on the tilt-wing model (ref. 8) indicated that the wind-tunnel interferences calculated in reference 2 overcorrected the data in extreme conditions. The use of the effective skew angle would have reduced the corrections somewhat for the tilt-wing model, too, and would have led to improved correlation.

## Comparison With Flight

In view of scale effects and differences in model detailing and the differing accuracies and types of corrections required, comparison between flight tests and wind-tunnel tests can be a particularly difficult task. This comparison is unusually difficult when the comparison is attempted in order to evaluate only one of the many effects that are being considered. Paper no. 5 by Kenneth W. Goodson, for example, showed that a 0.09-scale model suffered from large Reynolds number effects (fig. 6 of paper no. 5), but that a 0.60-scale model did yield reasonable results in predicting the maximum rate of descent for a four-propeller tilt-wing configuration. As noted in paper no. 5, the data for the 0.60-scale model were corrected for wall effects. The corrections used the effective skew angle and considered the effect of finite span. The correction,

as obtained in this manner, resulted in a change of flight-path angle of several degrees and substantially improved the correlation between results from the large model and flight data.

## Limit on Testing in Closed Wind Tunnels

Rae, of the University of Washington, by testing rotors in inserts in the UWAL 8- by 12-foot wind tunnel,[1] has shown that the wake, upon meeting the floor behind the model, spreads laterally on the floor, is turned upward by the sidewalls, and produces a flow pattern in the wind tunnel as indicated on the left-hand side of figure 13. Normally, this disturbance is too far behind the model to produce any discernible effect on the data. However, if the wake is deflected downward sharply enough, the recirculation pattern envelops the model and the data are severely affected. In the present case, the point of divergence occurs at an effective skew angle of 65° and produces a theoretical intersection of wake and floor about $2\frac{2}{3}$ spans behind the point of origin of the wake. This point agrees quite closely with the value obtained by Rae.

The close correlation between such widely divergent models (rotor and jet flap) and wind-tunnel configurations ($\gamma = 1.5$ and $\gamma = 0.7$) indicates two things. First, there is a finite lower limit to the test speed at which reliable and correctable data can be obtained in a closed wind tunnel; and, second, this limit is not seriously affected by model configuration but is largely determined only by the size of the vertical-lift elements of the model. This limiting effect is still relatively unexplored. It may be that certain wind-tunnel configurations will be affected differently from others. It further seems possible that if the model configuration were extremely long, or if the lifting elements were disposed over a large longitudinal distance, the limiting speed could be adversely affected. Substantial additional experimental work will be required in order to define these (and similar) effects.

Actually, the onset of this limiting lower speed follows a rule rather similar to that presented in paper no. 25 by Thomas R. Turner, in which it is noted that a moving belt is required in order to simulate ground effect when the combination of lift coefficient and height above the ground produces an intersection of effective wake and floor which is less than $2\frac{1}{2}$ spans behind the model. Thus, the boundary layer on the walls is probably a major causative factor in producing these recirculation effects. The study of a number of boundary-layer control features is indicated in the hope that significant gains could be obtained.

As stated previously, the study of limiting forward speeds for VTOL tests in wind tunnels is still in an early stage and, consequently, large uncertainties are present. In view of this uncertainty, a value of 3 spans is suggested

---

[1]Rae, William H., Jr.: An Experimental Investigation of the Maximum Size Rotor That Can be Tested in a Rectangular Wind Tunnel. Grant No. DA-ARO(D)-31-124-G481 (U.S. Army Res. Office, Durham, N.C.), Jan. 5, 1966.

as an adequately accurate number to use in deciding the speed above which full confidence in the data is justified. In considering the span of the model, it should be adequate to consider only the span of the vertical-lift elements of the configuration.

It might be noted that there could be two ways of locating this limit. In the present paper, the wake vorticity is assumed to be responsible for the circulatory flow around the wind-tunnel walls. An alternative viewpoint is that the circulatory flow is a result merely of the wake mass flow dividing at the tunnel floor. If so, the proper skew angle to use for the limit would be the original or momentum-value skew angle, and the corresponding limit would be an intersection of wake and floor just $1\frac{1}{4}$ spans behind the model. At the present time, insufficient experimental evidence exists and therefore a choice between the two concepts is difficult.

## Size of Models

The real limitation on the allowable size of a model is not really the absolute size of the correction which will be engendered by testing a given size model in a given wind tunnel. Instead, the limitations on model size are defined largely by the variation of the wall-induced interference over the extent of the model. As pointed out previously, this variation can be considered in terms of effective aerodynamic distortion (such as twist and camber) of the model. The maximum size model that can be used, therefore, is determined by the extent to which the effect of such distortions can be determined. For simple isolated wings, as well as for isolated rotors and propellers, such effects can be determined with reasonable accuracy, and relatively large models may be accepted. For more exotic means of producing lift, as well as for many interacting combinations of simple elements, the prediction of the effect of these interference distortions is doubtful at best. In such cases, it may be necessary to limit the size of VTOL models to one-quarter to one-third of the wind-tunnel width if accurate, reliable results are desired.

On the other hand, scale effects and the physical size limitations in providing small powered models may override considerations of wall effects. Thus the eventual sizing of a particular model will be the result of many engineering compromises and the overall accuracy of predication of full-scale flight characteristics will be determined by the degree to which such compromises are optimized.

## Application to Langley Data

The close correlation of data from different wind tunnels, both in this paper and in references 8 to 10, as a result of applying the corrections of reference 2 is quite encouraging. As a result, the decision has been made to incorporate these corrections into all new VTOL data from the Langley 300-MPH 7- by 10-foot tunnel at the earliest possible date.

## Wind-Tunnel Configurations for Small Wall Effects

As indicated in the foregoing sections of this paper, wall effects can be large and troublesome in a closed wind tunnel; however, a large degree of relief can be obtained by the use of wind tunnels with mixed boundaries. An example, suggested by Ray H. Wright of the Langley Research Center, is shown in figure 14. In this example, the wind tunnel is 1.5 times as deep as it is wide, has an open lower boundary, a closed upper boundary, and slotted sidewalls.

The classical correction factor (eq. (1)) for a vanishingly small model in this wind tunnel has been calculated and is also presented in figure 14 as a function of the percentage of the sidewalls that is opened by the slots. The correction factor is observed to fall very rapidly for very small slot openings. The curve then becomes less sensitive to slot opening, and the correction factor becomes zero with a 5-percent slot opening.

This calculation was made for a wake which passes directly rearward without deflection. In order to determine the effect of deflecting the wake, the small (2.70' × 1.88') wind tunnel was built. Extensive tests have been conducted on the jet-flap model previously described. A sample of the results is shown in figure 15. At a momentum coefficient of 3.0, the wall effects on the model lift are essentially negligible (fig. 15(a)). However, wall effects at the tail are not zero (fig. 15(b)). Despite the large scatter, there seems to be some, but certainly not total, relief from wall effects at the tail.

At the highest momentum coefficient ($C_\mu$ = 10.0), the boundary effects on the tail are far more severe (fig. 16). Figure 16 shows that the wind tunnel with mixed boundaries leads to measurements less accurate than even those from the small closed wind tunnel. This effect is believed to be due to the gross disruption of the tunnel flow resulting from the large spillage of air from the lower open boundary of the tunnel.

Despite the fact that a zero-correction wind tunnel for VTOL testing has not been achieved as yet, the results obtained to date are sufficiently encouraging so that work on several slotted wind tunnels is continuing. This work is being expanded to include several other low-correction wind tunnels such as the closed-on-bottom-only configurations.

## CONCLUSIONS

This study of the application of jet-boundary corrections to VTOL wind-tunnel data indicates the following conclusions:

1. The skew angle used in applying the corrections of NASA TR R-124 to VTOL data should be such that the angular deflection of the wake vorticity from the horizontal is essentially one-half of the wake deflection obtained from momentum theory at the lifting element.

2. When the effective skew angle is used, the corrections of NASA TR R-124 provide greatly improved agreement between the data obtained in different wind tunnels, not only for lift, but also for pitching moment and tail normal force.

3. For accurate corrections, it is necessary to include the effects of finite model span, at least when the model span is on the order of one-half the wind-tunnel width.

4. There appears to be a lower limit to the test speed at which reliable and correctable results can be obtained from closed wind tunnels. In view of present uncertainties, it is suggested that this limit be taken as an intersection of effective wake and floor that is three times the span of the vertical-lift system behind the wake origin.

5. Considerable alleviation of boundary effects may be obtained by the use of wind tunnels employing mixed boundaries.

## REFERENCES


1. Theodorsen, Theodore: The Theory of Wind-Tunnel Wall Interference. NACA Rept. 410, 1931.

2. Heyson, Harry H.: Linearized Theory of Wind-Tunnel Jet-Boundary Corrections and Ground Effect for VTOL-STOL Aircraft. NASA TR R-124, 1962.

3. Heyson, Harry H.: Wind-Tunnel Wall Interference and Ground Effect for VTOL-STOL Aircraft. J. Am. Helicopter Soc., vol. 6, no. 1, Jan. 1961, pp. 1-9.

4. Heyson, Harry H.: Tables of Interference Factors for Use in Wind-Tunnel and Ground-Effect Calculations for VTOL-STOL Aircraft. Part I - Wind Tunnels Having Width-Height Ratio of 2.0. NASA TN D-933, 1962.

5. Heyson, Harry H.: Tables of Interference Factors for Use in Wind-Tunnel and Ground-Effect Calculations for VTOL-STOL Aircraft. Part II - Wind Tunnels Having Width-Height Ratio of 1.5. NASA TN D-934, 1962.

6. Heyson, Harry H.: Tables of Interference Factors for Use in Wind-Tunnel and Ground-Effect Calculations for VTOL-STOL Aircraft. Part III - Wind Tunnels Having Width-Height Ratio of 1.0. NASA TN D-935, 1962.

7. Heyson, Harry H.: Tables of Interference Factors for Use in Wind-Tunnel and Ground-Effect Calculations for VTOL-STOL Aircraft. Part IV - Wind Tunnels Having Width-Height Ratio of 0.5. NASA TN D-936, 1962.

8. Grunwald, Kalman J.: Experimental Study of Wind-Tunnel Wall Effects and Wall Corrections for a General-Research V/STOL Tilt-Wing Model With Flap. NASA TN D-2887, 1965.

9. Davenport, Edwin E.; and Kuhn, Richard E.: Wind-Tunnel-Wall Effects and Scale Effects on a VTOL Configuration With A Fan Mounted in the Fuselage. NASA TN D-2560, 1965.

10. Lee, Jerry Louis: An Experimental Investigation of the Use of Test Section Inserts as a Device To Verify Theoretical Wall Corrections for a Lifting Rotor Centered in a Closed Rectangular Test Section. M. S. Thesis, Univ. of Washington, Aug. 20, 1964.

11. Staff of Powered-Lift Aerodynamics Section, NASA Langley Res. Center: Wall Effects and Scale Effects in V/STOL Model Testing. AIAA Aerodynamic Testing Conf., Mar. 1964, pp. 8-16.

12. Heyson, Harry H.; and Katzoff, S.: Induced Velocities Near a Lifting Rotor With Nonuniform Disk Loading. NACA Rept. 1319, 1957. (Supersedes NACA TN 3690 by Heyson and Katzoff and TN 3691 by Heyson.)

13. Joppa, R. G.: Experimental and Theoretical Investigation of Wind Tunnel Geometry, Emphasizing Factors Pertinent to V/STOL Vehicles Testing. Progr. Rept. No. 2 (NASA Grant NGR-48-002-010), Univ. of Washington, Jan. 15, 1966.

14. Cone, Clarence D., Jr.: A Theoretical Investigation of Vortex-Sheet Deformation Behind a Highly Loaded Wing and Its Effect on Lift. NASA TN D-657, 1961.

15. Heyson, Harry H.: Nomographic Solution of the Momentum Equation for VTOL-STOL Aircraft. NASA TN D-814, 1961. (See also "V-STOL Momentum Equation," Space/Aeron., vol. 38, no. 2, July 1962, pp. B-18 — B-20.)

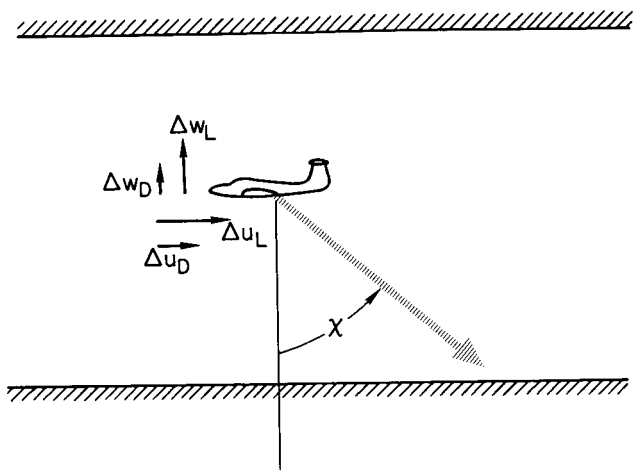


Figure 1.- Notation and positive direction of interference velocities and skew angle used in correction theory of NASA TR R-124.

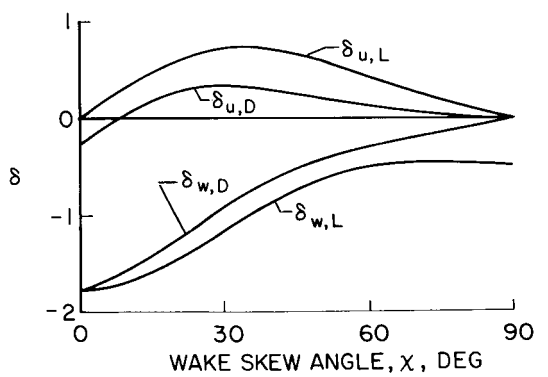


Figure 2.- Typical behavior of correction factors as a function of wake skew angle. Closed tunnel; $\frac{B}{H} = 1.5$.

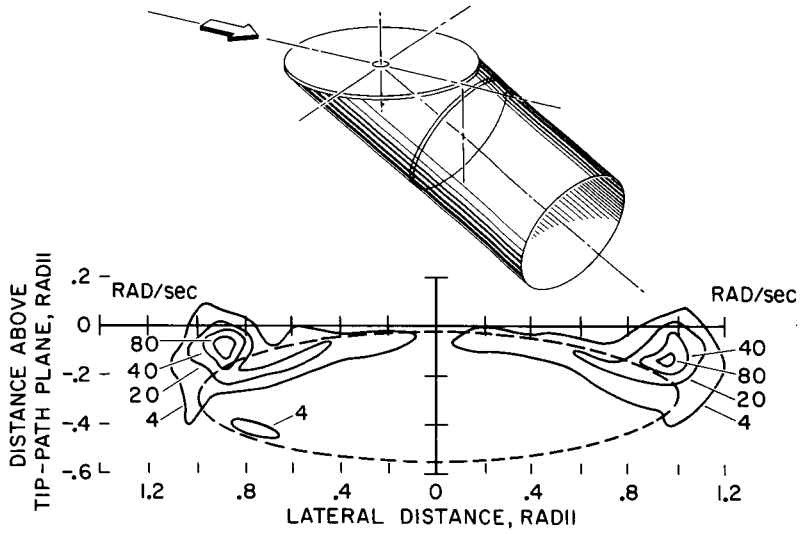


Figure 3.- Vorticity distribution measured at x = 0.07R behind the trailing edge of a lifting rotor. $\chi = 75^{0}$.

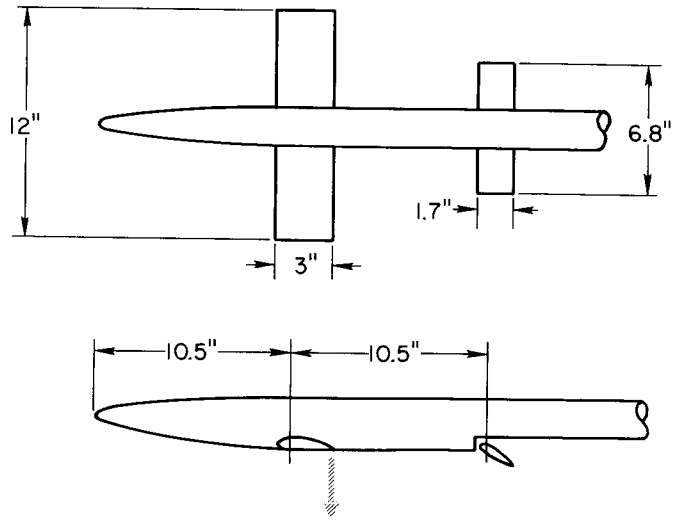


Figure 4.- Jet-flap model.

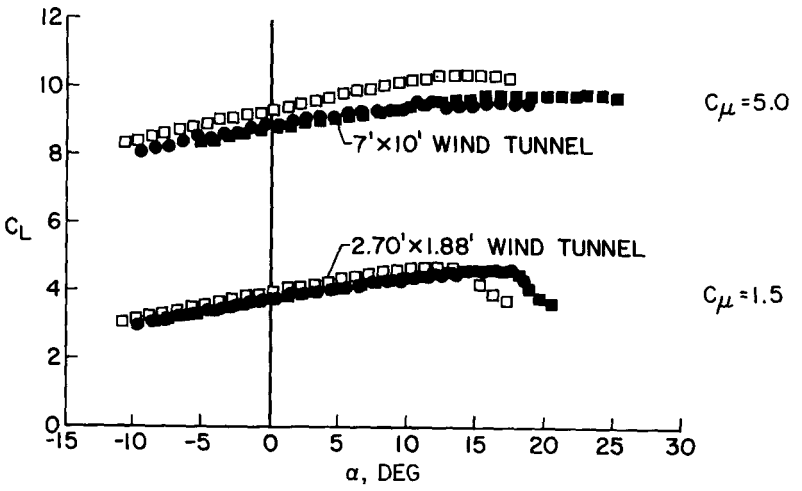


(a) Lift coefficient $C_L$.

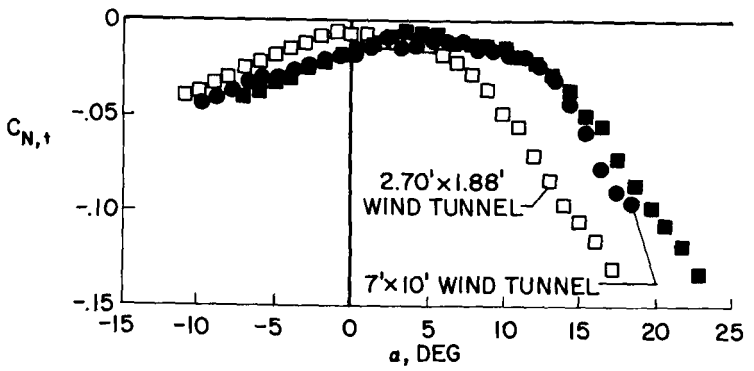


(b) Tail-normal-force coefficient $C_{N,t}$. $C_\mu$ = 5.0; tail incidence, 21.6°.

Figure 5.- Comparative data for jet-flap model tested in two different closed wind tunnels. Solid symbols denote values corrected by using $X_{eff}$; correction factors include effect of finite span of both wing and tail.

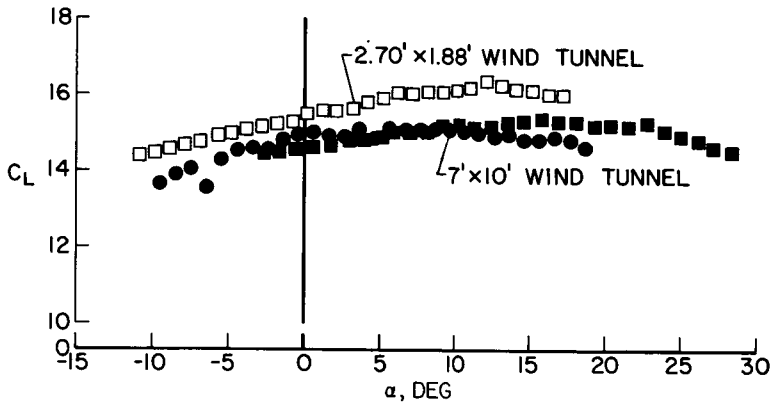


(a) Lift coefficient $C_L$.

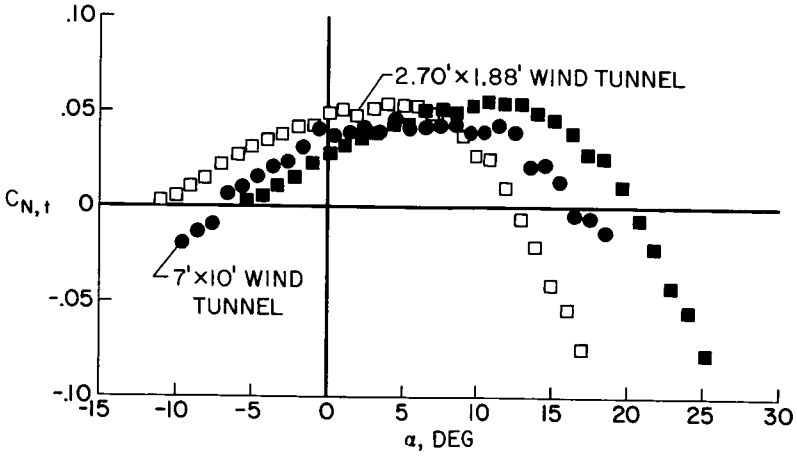


(b) Tail-normal-force coefficient $C_{N,t}$. Tail incidence, 29°.

Figure 6.- Comparative data for jet-flap model at $C_\mu = 10.0$ tested in two different closed wind tunnels. Solid symbols denote values corrected by using $X_{eff}$; correction factors include effect of finite span of both wing and tail.

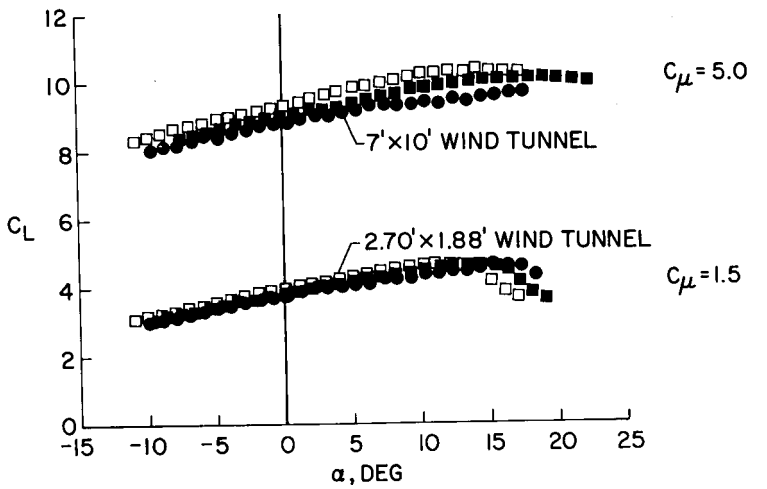


(a) Lift coefficient $C_L$.

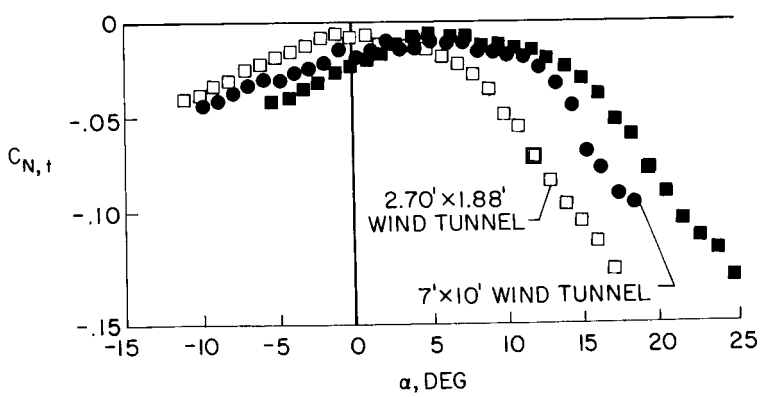


(b) Tail-normal-force coefficient $C_{N,t}$. $C_\mu$ = 5.0; tail incidence, 21.6°.

Figure 7.- Comparative data for the jet-flap model tested in two different closed wind tunnels. Solid symbols denote values corrected by using $X_{eff}$; correction factors for a zero-span model.

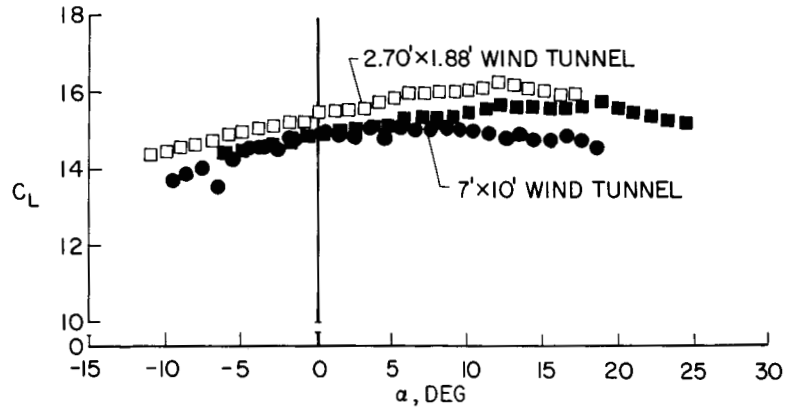


(a) Lift coefficient $C_L$.

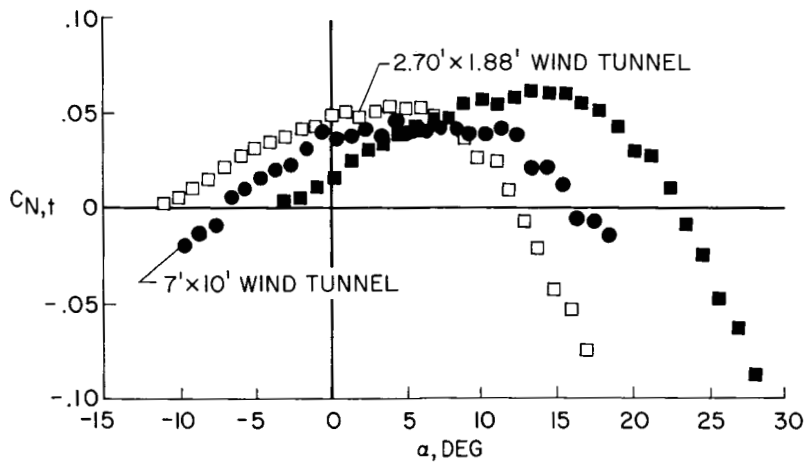


(b) Tail-normal-force coefficient $C_{N,t}$. Tail incidence, $29^0$.

Figure 8.- Comparative data for the jet-flap model at $C_\mu = 10.0$ in two different closed wind tunnels. Solid symbols denote values corrected by using $\chi_{eff}$; correction factors for a zero-span model.

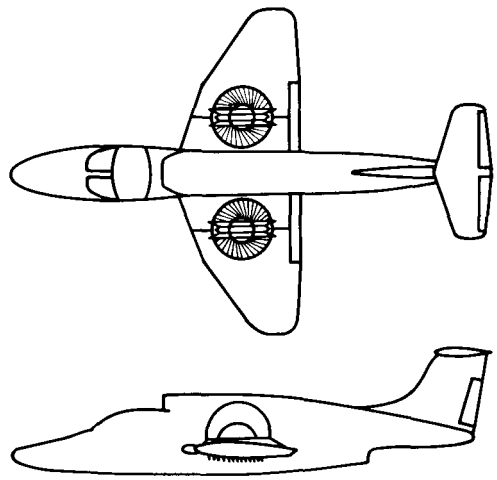

Figure 9.- Sketch of fan-in-wing model.

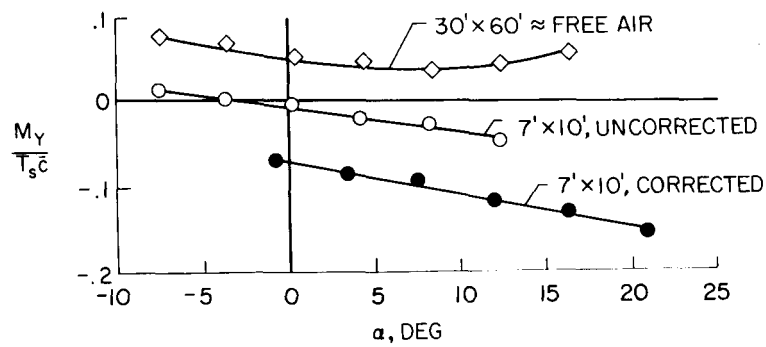


Figure 10.- Comparison of pitching-moment data obtained in two wind tunnels with fan-in-wing model. Corrections have been applied by using method of NASA TR R-124 with the original skew angle. $\frac{V}{V_{j,s}} = 0.48$; exit-louver angle, $0^{o}$.

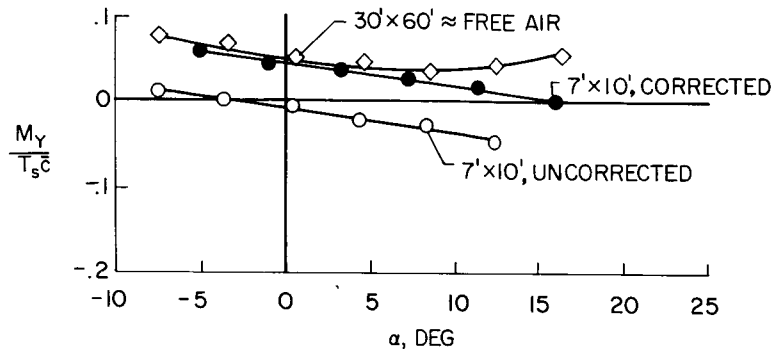


Figure 11.- Comparison of pitching-moment data obtained in two wind tunnels with fan-in-wing model. Corrections have been applied by using method of NASA TR R-124 with effective skew angle. $\frac{V}{V_{j,s}} = 0.48$; exit-louver angle, $0^0$.

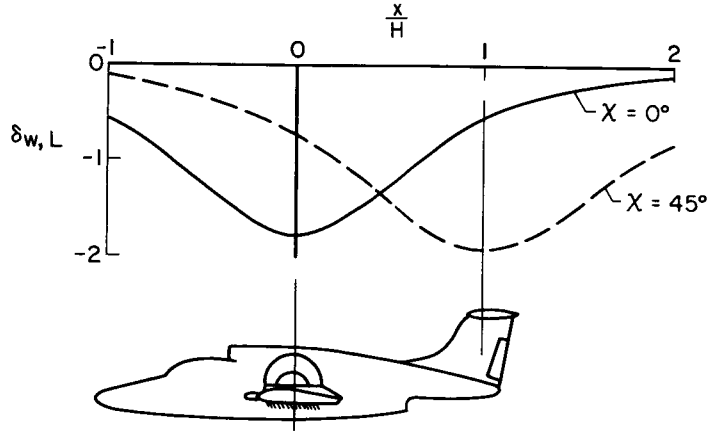


Figure 12.- Variation of vertical interference due to lift $(\delta_{w,L})$ along the longitudinal axis of fan-in-wing model.

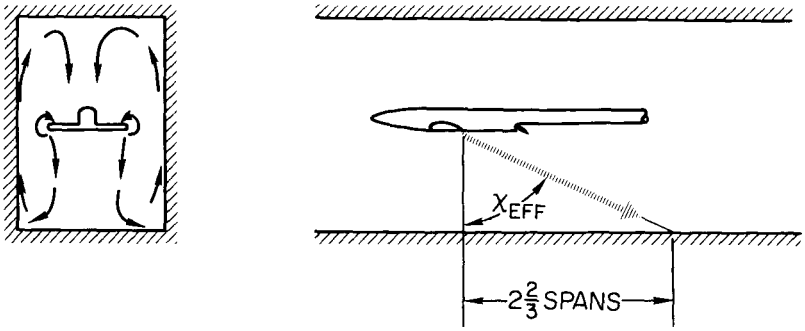


Figure 13.- Sketch of flow behind model in a closed wind tunnel, and limit found in tests of jet-flap model.

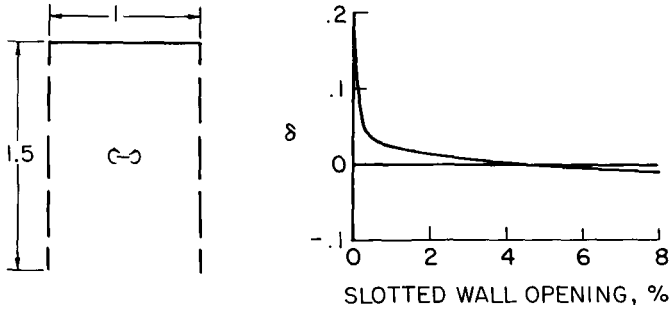


Figure 14.- Calculated classical correction factors for a wind tunnel with mixed boundaries. Model is assumed to be vanishingly small.

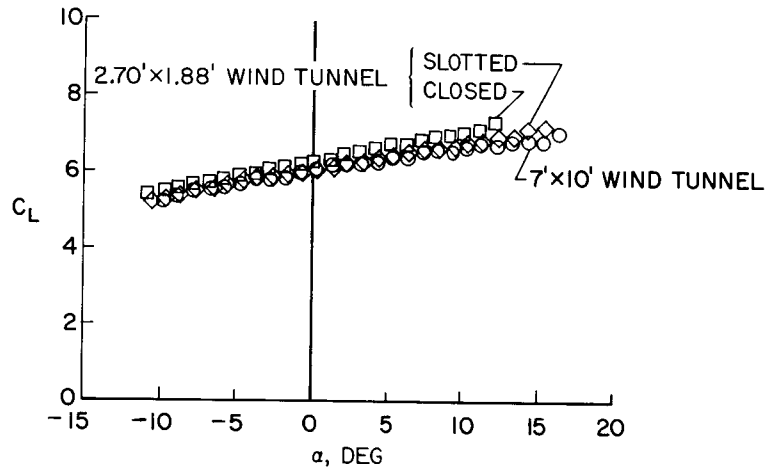


(a) Lift coefficient $C_L$.

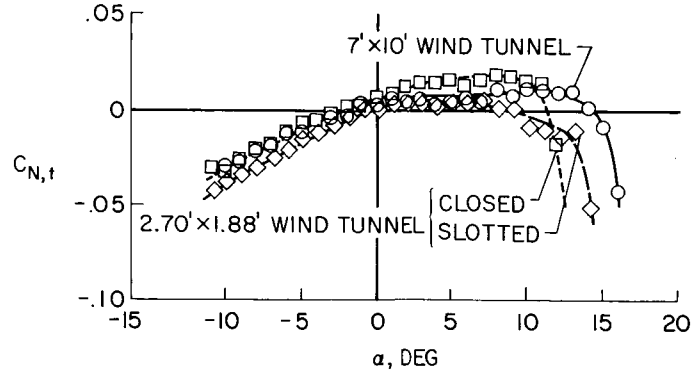


(b) Tail-normal-force coefficient $C_{N,t}$.

Figure 15.- Comparison of data obtained in three wind tunnels for jet-flap model at $C_\mu = 3.0$.

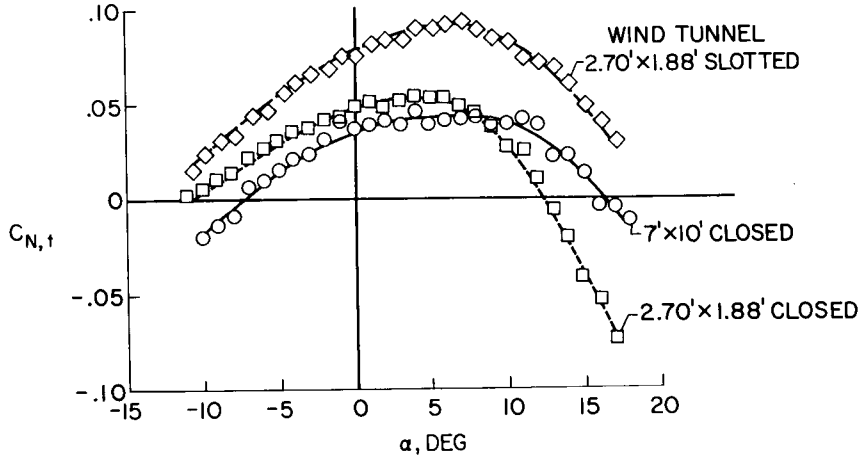


Figure 16.- Comparative data on tail-normal-force coefficient for jet-flap model at $C_\mu = 10.0$ in three different wind tunnels.